bioRxiv preprint doi: https://doi.org/10.1101/102517; this version posted January 24, 2017. The copyright holder for this preprint (which was not certified by peer review) is the author/funder, who has granted bioRxiv a license to display the preprint in perpetuity. It is made available under aCC-BY-NC-ND 4.0 International license.

Medicago truncatula MOT1.3 is a plasma membrane molybdenum transporter required for nitrogenase activity in root nodules.

Manuel Tejada-Jiménez[a1,2], Patricia Gil-Díez[a], Javier León-Mediavilla[a], Jiangqi Wen[b], Kirankumar S. Mysore[b], Juan Imperial[a,c], Manuel González-Guerrero[a,1]

[a]Centro de Biotecnología y Genómica de Plantas (UPM-INIA). Campus de Montegancedo. Universidad Politécnica de Madrid. Crta. M-40 km 38. 28223 Pozuelo de Alarcón (Madrid). Spain.

[b]Plant Biology Division, The Samuel Roberts Noble Foundation, Ardmore, Oklahoma 73401.

[c]Consejo Superior de Investigaciones Científicas. Madrid. Spain.

[1]Address correspondence: Manuel Tejada-Jiménez (q62tejim@uco.es) and Manuel González-Guerrero (manuel.gonzalez@upm.es)

[2]Present address: Department of Biochemistry and Molecular Biology. Universidad de Córdoba. Campus de Rabanales. Edificio Severo Ochoa. Córdoba. Spain.

bioRxiv preprint doi: https://doi.org/10.1101/102517; this version posted January 24, 2017. The copyright holder for this preprint (which was not certified by peer review) is the author/funder, who has granted bioRxiv a license to display the preprint in perpetuity. It is made available under aCC-BY-NC-ND 4.0 International license.

Abstract

Molybdenum has a critical role in biological nitrogen fixation since nitrogenase activity, the central enzyme of this process, requires the presence of this element in its active center. Therefore, any strategy of sustainable agriculture based on biological nitrogen fixation as nitrogen source for crops, requires an efficient molybdenum supply to the nitrogen-fixing tissues. However, in legumes, where symbiotic nitrogen fixation takes place, transporters mediating molybdenum transport have not been identified so far. Here, we report the *Medicago truncatula* molybdate transporter MtMOT1.3 as responsible for molybdenum supply for symbiotic nitrogen fixation. MtMOT1.3 is a member of the molybdate transporter family MOT1, and the only member of this family in *M. truncatula* showing a nodule-specific expression. Immunolocalization studies revealed that MtMOT1.3 is expressed in the plasma membrane of nodule cells where nitrogen fixation occurs. A *mot1.3* knockout mutant showed an impaired growth concomitant with a reduction in nitrogenase activity. This phenotype was rescued upon addition of an assimilable nitrogen source or, under nitrogen-limiting conditions, by increasing molybdate concentrations in the nutritive solution. Furthermore, *mot1.3* mutant plants transformed with a functional copy of *MtMOT1.3* showed a wild type-like phenotype. These results are important to understand how legumes supply molybdenum for symbiotic nitrogen fixation

bioRxiv preprint doi: https://doi.org/10.1101/102517; this version posted January 24, 2017. The copyright holder for this preprint (which was not certified by peer review) is the author/funder, who has granted bioRxiv a license to display the preprint in perpetuity. It is made available under aCC-BY-NC-ND 4.0 International license.

Introduction

Molybdenum is one of the scarcest oligonutrients in the biosphere (Esteifel, 2002). Plants use it as part of the molybdenum cofactor (Moco) in just five enzymes involved in nitrate assimilation, purine metabolism, phytohormone production, and sulfite detoxification (Tejada-Jimenez et al., 2013). This nutrient, unlike other transition metals, is recovered from soil as the oxyanion molybdate instead of a cationic form. This determines that the transporters involved in this process are not the classical ones required for iron, copper, or zinc uptake, but members of other families. Molybdate shares some physicochemical characteristics with sulfate leading to cross-inhibition of sulfate transport by molybdate, probably due to non-specific molybdate transport through sulfate transporters in plants (Stout et al., 1951). Therefore, until recently it was thought that sulfate transporters might mediate molybdate transport in eukaryotic systems (Mendel and Hansch, 2002; Kaiser et al., 2005). The only known plant-type specific molybdate transporters belong to the Molybdate Transporter type 1 (MOT1) family and were identified in parallel in the green alga *Chlamydomonas reinhardtii* (Tejada-Jimenez et al., 2007) and in the higher plant *Arabidopsis thaliana* (Tomatsu et al., 2007). They share a high degree of homology with the sulfate transport family SULTR, but lack the conserved STAS domain (Tejada-Jimenez et al., 2007). In *C. reinhardtii*, CrMOT1 is responsible for high-affinity molybdate uptake, a process that is not severely affected by sulfate, indicating that MOT1 proteins are molybdate-specific transporters (Tejada-Jimenez et al., 2007). In Arabidopsis two members of the MOT1 family have been identified. One of them has been proposed to play a role in efficient Mo uptake from the soil (Tomatsu et al., 2007), although this function is not clear given the conflicting subcellular localizations reported for this transporter in plasma membrane or in mitochondria (Tomatsu et al., 2007; Baxter et al., 2008); while a second member of the MOT1 family is located in the vacuole of leaves and seems to be involved in intracellular and inter-organ Mo transport (Gasber et al., 2011). More recently, a MOT1 protein (LjMOT1) has been identified in *Lotus japonicus*, with a role in molybdate uptake from soil and translocation to the shoots, being located in the plasma membrane when expressed in tobacco leaves (Gao et al., 2016). In addition, another molybdate transporter family, MOT2, belonging to the major facilitator superfamily has been identified in *C. reinhardtii* (Tejada-Jimenez et al., 2011), indicating that molybdate

bioRxiv preprint doi: https://doi.org/10.1101/102517; this version posted January 24, 2017. The copyright holder for this preprint (which was not certified by peer review) is the author/funder, who has granted bioRxiv a license to display the preprint in perpetuity. It is made available under aCC-BY-NC-ND 4.0 International license.

transporters have appeared at least twice in evolution. However, its functionality as molybdate transporters has only been proved in this alga.

While all the plants employ molybdenum for Moco biosynthesis, legumes have an additional use for it. These organisms also require molybdenum for the assembly of the iron-molybdenum cofactor (FeMoco) of nitrogenase (Georgiadis et al., 1992; Rubio and Ludden, 2008), the enzyme responsible for nitrogen fixation in their root nodules. In legumes, FeMoco is assembled by diazotrophic bacteria living within differentiated root organs, the nodules. These organs are developed in a complex process starting with the detection of rhizobial nodulation factors (Nod) by the host plant that leads to root hair curling, bacteria trapping, hydrolysis of the plant cell wall and bacteria delivery to the root nodule primordium through an infection thread (Kondorosi et al., 1984; Brewin, 1991; Oldroyd, 2013). Once in the plant cytoplasm, rhizobia together with a plant-derived membrane result in organelle-like structures, the symbiosomes, where nitrogen fixation takes place. Two different types of nodules can be found in legumes (Sprent, 2007): determinate and inderterminate nodules. In inderterminate nodules, as those found in *Medicago truncatula*, the continuous meristem growth results in the formation of at least four different zones in mature nodules: the meristematic zone that drives nodule growth; the infection/differentiation zone, where rhizobia are released through the infection thread and differentiates to bacteroids; the fixation zone where nitrogenase carries out its enzymatic activity; and the senescent zone where bacteroids are degraded (Vasse et al., 1990). An additional nodule zone, the interzone, can be defined as the transition between infection/differentiation and fixation zone (Roux et al., 2014). Once the oxygen tension drops in the interzone, endosymbiotic bacteroids express nitrogenase and the machinery that allows them synthesize FeMoco. Among them, is the *modABC* operon, responsible for molybdate uptake from the peribacteroid space (Maupin-Furlow et al., 1995; Delgado et al., 2006; Hernandez et al., 2009). Consequently, for molybdate to reach the bacteroids, it has to cross the plasma and the symbiosome membranes, a process that has to be mediated by transporters belonging to two different families, given the two different directions of transport required.

In spite of the essential role that molybdenum has in nitrogenase, and the importance of nitrogenase in legume colonization of new environments and in sustainable

bioRxiv preprint doi: https://doi.org/10.1101/102517; this version posted January 24, 2017. The copyright holder for this preprint (which was not certified by peer review) is the author/funder, who has granted bioRxiv a license to display the preprint in perpetuity. It is made available under aCC-BY-NC-ND 4.0 International license.

agriculture, the transporters involved in molybdenum supply to the bacteroids are not known. It can be hypothesized that molybdate transfer could in some cases be mediated by sulfate transporters. In this case, molybdate transfer across the symbiosome membrane could be carried out by SST1-like proteins, that have been previously associated with sulfate delivery to symbiosomes (Krusell et al., 2005). At the plasma membrane, another sulfate transporter, such a SHST1 homologue could mediate molybdate uptake by rhizobia-infected cells since this transporter from the legume *Stylosanthes hamata* has already been shown to transport molybdate when it is expressed in yeast (Fitzpatrick et al., 2008). However, *in planta* SHST1 is expressed in the root and it is involved in sulfate uptake (Smith et al., 1995), while its relationship with plant molybdate transport has not been determined yet. A more likely alternative would be transporters from the MOT1 or MOT2 families, since they could finely tune molybdate delivery for symbiotic nitrogen fixation, given their high specificity for this anion.

In this work, we have identified a *M. truncatula* member of the MOT1 family (MtMOT1.3) involved in molybdate transport to nodule cells. *MtMOT1.3* is specifically expressed in nodules. Its protein product is located in the plasma membrane of infected and non-infected cells in the fixation zone of the nodule, coinciding with the zone where *MtMOT1.3* is expressed. *M. truncatula* plants lacking a functional *MtMOT1.3* gene show a reduction of nitrogenase activity connecting MtMOT1.3 function with molybdenum supply for FeMoCo biosynthesis. This is the first molybdate transporter known to be specific of legume symbiotic nitrogen fixation.

Results

MtMoT1.3 belongs to the molybdate transporter MOT1 family and is specifically expressed in nodules.

Due to the possible role of MOT1 transporters in Mo supply for symbiotic nitrogen fixation, we carried out a search for MOT1 members in the *M. truncatula* genome. Five putative *M. truncatula* proteins were found (encoded by *Medtr1g010210*, *Medtr1g010270*, *Medtr3g464210*, *Medtr4g011600* and *Medtr3g108190*) showing a sequence identity between 51.4 % and 65.7 % with an Arabidopsis member of the MOT1 family. These proteins were annotated as sulfate transporter-like proteins; however, sequence comparison

bioRxiv preprint doi: https://doi.org/10.1101/102517; this version posted January 24, 2017. The copyright holder for this preprint (which was not certified by peer review) is the author/funder, who has granted bioRxiv a license to display the preprint in perpetuity. It is made available under aCC-BY-NC-ND 4.0 International license.

showed that they cluster with plant MOT1 proteins and are more distant to sulfate transporters (SULTR) (Figure 1A). Additionally, these proteins also contain the two sequence motifs conserved in all MOT1 proteins (Tejada-Jimenez et al., 2007) (Figure 1B). Therefore, we named these proteins MtMOT1.1 to MtMOT1.5, respectively. The number of MOT1 members present in *M. truncatula* contrasts with the situation reported for Arabidopsis where only two MOT1 transporters are present (Tomatsu et al., 2007; Baxter et al., 2008; Gasber et al., 2011). Analysis of the number of MOT1 members in already sequenced plants showed that these proteins are present, in average, in a higher number in legumes than in non-legumes plants (Supplemental Table 1). This finding suggests a particular role of MOT1 proteins in legumes, where an additional molybdenum sink is present: diazotrophic bacteria in root nodules.

In order to study the possible relationship of the five putative MOT1 members of *M. truncatula* with symbiotic nitrogen fixation, a transcriptional analysis of these genes was carried out by real-time RT-PCR in plants during symbiotic association with *Sinorhizobium meliloti* or in uninoculated plants fertilized with nitrogen. We found that *MtMOT1.3* expression is restricted to the nodule (Figure 1C and 1D), while transcripts from the other four *MtMOT1* genes were also detected at varying levels in other organs of the analyzed plants (Supplemental Figure 1). These results strongly suggest an important role of MtMOT1.3 in the nodule, likely in molybdate transport connected to symbiotic nitrogen fixation. *MtMOT1.3* expression levels were not significantly affected by molybdate concentration in the nutritive solution (Supplemental Figure 2).

MtMOT1.3 is a molybdate transporter

All the MOT1 proteins reported so far mediate molybdate transport, in form of the oxyanion molybdate, to the cytosol (Tejada-Jimenez et al., 2013). The high sequence similarity that MtMOT1.3 shares with the already characterized molybdate transporters suggests that this protein could also mediate molybdate transport in the same direction. To test this hypothesis, *MtMOT1.3* was heterologously expressed in the yeast *Saccharomyces cerevisiae*. This yeast is a good model to study of Mo transporters since it is one of the few organisms that do not use molybdenum, excluding any effect of endogenous specific molybdate transport activity (Mendel and Bittner, 2006). Toxicity studies showed that

bioRxiv preprint doi: https://doi.org/10.1101/102517; this version posted January 24, 2017. The copyright holder for this preprint (which was not certified by peer review) is the author/funder, who has granted bioRxiv a license to display the preprint in perpetuity. It is made available under aCC-BY-NC-ND 4.0 International license.

yeasts expressing *MtMOT1.3* exhibit a defective growth in synthetic dextrose (SD) solid medium in the presence of 50 µM molybdate, compared with yeast transformed with the empty vector pDR196, but no growth differences were observed with the control when no additional molybdate was added to the growth medium (Figure 2A). Similar results were obtained in SD liquid medium by monitoring yeast growth along the time (Figure 2B, Supplemental Figure 3). The toxic effect observed in yeast is the likely result of molybdenum being transported and accumulated in the cell as a result of MtMOT1.3 activity (Figure 2C). This result supports the functionality of MtMOT1.3 as molybdate transporter towards the cytosol.

MtMOT1.3 is expressed in the plasma membrane of nodule cells of the interzone and fixation zones

To investigate the role of MtMOT1.3 in molybdenum supply to the nodule, we studied the tissue specific localization of *MtMOT1.3* expression. This was assessed by analyzing the expression of the ß-glucoronidase (*gus*) gene under the control of 1.1 kb of genomic DNA directly upstream of the *MtMOT1.3* starting codon, that was selected as promoter. Using this genetic construct, GUS activity was found in the nodule interzone, with the maximum in the area corresponding with the fixation zone (Figure 3A and 3B). This expression distribution within the nodule matches with the transcription data available in the Symbimics database obtained by means of laser-capture microdissection coupled to RNA sequencing (Roux et al., 2014), where *MtMOT1.3* expression is mainly detected in the interzone and fixation zones (Figure 3C).

Localization of MtMOT1.3 protein was also analyzed using an immunohistochemical and confocal microscopy approach. *M. truncatula* plants were transformed with a genetic construct comprising the genomic region of *MtMOT1.3* fused in frame with three hemagglutinin (HA) epitopes in C-terminus (MtMOT1.3-HA), under the control of the same promoter used for the GUS assay. The chimeric MtMOT1.3-HA protein was detected (in the red channel) with a mouse anti-HA antibody and an Alexa594-conjugated anti-mouse secondary antibody. Its position within the nodule was traced by DNA staining using 4',6-diamino-phenylindole (DAPI) (blue) and a *S. meliloti* strain constitutively expressing GFP (green). In agreement with the GUS activity data,

bioRxiv preprint doi: https://doi.org/10.1101/102517; this version posted January 24, 2017. The copyright holder for this preprint (which was not certified by peer review) is the author/funder, who has granted bioRxiv a license to display the preprint in perpetuity. It is made available under aCC-BY-NC-ND 4.0 International license.

MtMOT1.3-HA was detected in the interzone and fixation zones of the nodule (Figures 4A to 4C). Particularly, MtMOT1.3-HA signal was found in the periphery of infected and non-infected cells (Figures 4D to 4F), fitting with plasma membrane localization. This signal was not the result of autofluorescence, since sections obtained from the same biological material, subjected to the same preparation protocol with the exception of the incubation with the primary anti-HA antibody, did not show any fluorescence in the Alexa594 emission spectrum (Supplemental Figure 4). Moreover, the specific peripheral distribution of MtMOT1.3-HA was also observed using an Alexa488-conjugated secondary antibody in nodules containing m-Cherry-expressing *S. meliloti* (Supplemental Figure 5A-5B). No MtMOT1.3-HA signal was detected by Western blot analyses in roots from nodulated plants (Supplemental Figure 6), consistent with the nodule-specifc expression data obtained by real-time PCR. To confirm the subcellular localization of MtMOT1.3 in the plasma membrane, its coding sequence fused to the green fluorescent protein (GFP) in C-terminus was transiently expressed in *Nicotiana benthamiana* leaves together with a plasma membrane marker fused to cyan fluorescent protein (CFP). MtMOT1.3 signal and plasma membrane marker signal co-localized in *N. benthamiana* leaves cells expressing both genetic constructs (Figure 4G to 4I), supporting the localization of MtMOT1.3 in the plasma membrane. However, no GFP or CFP signals were found in cells expressing only the plasma membrane marker or MtMOT1.3, respectively (Supplemental Figure 7), thus ruling out any non-specific signal when both constructs are co-expressed.

Lack of *MtMOT1.3* leads to a reduction of nitrogenase activity

In order to investigate the role of MtMOT1.3 in symbiotic nitrogen fixation, the mutant line NF10801 (*mot1.3-1*) was identified by a reverse genetics screening (Cheng et al., 2011; Cheng et al., 2014) from a *Transposable Element from Nicotiana tabacum* (*Tnt1*) insertion mutant library (Tadege et al., 2008). The mutant *mot1.3-1* carries a *Tnt1* insertion in the second exon of the *MtMOT1.3* gene at position +1782 from the starting codon (Figure 5A). *MtMOT1.3* transcripts were not detected in the homozygous *mot1.3-1* mutant (Figure 5B), therefore MtMOT1.3 activity is not present in this mutant line.

The phenotype of *mot1.3-1* was evaluated in symbiotic conditions, with nitrogen fixation as the sole nitrogen source, and under low Mo availability. In these conditions,

bioRxiv preprint doi: https://doi.org/10.1101/102517; this version posted January 24, 2017. The copyright holder for this preprint (which was not certified by peer review) is the author/funder, who has granted bioRxiv a license to display the preprint in perpetuity. It is made available under aCC-BY-NC-ND 4.0 International license.

mot1.3-1 mutant showed a reduced growth rate compared with wild-type plants (Figure 5C). Consequently, plant biomass was reduced in the *mot1.3-1* mutant by 70 % in shoots and 55 % in roots (Figure 5D). Nitrogenase activity was measured in *mot1.3-1* and wild-type plants by the acetylene-reduction assay (Dilworth, 1966; Schöllhorn and Burris, 1966). *mot1.3-1* plants showed a reduction of 90 % in nitrogenase activity, as compared to the activity measured in wild-type plants (Figure 5E). Nodulation was not affected in the *mot1.3-1* mutant, since nodules were comparable to wild-type plants in terms of number and shape (Figure 5F and 5G). Moreover, no differences in nodule anatomy, or nodulation kinetics were observed between mutant and control plants (Supplemental Figure 8). However, these nodules were on average smaller than those from wild type plants (Figure 5G, Supplemental Figure 9). In addition, nodule molybdenum content in *mot1.3-1* plants was significantly higher than the control (Figure 5H), indicative of a role on molybdenum homeostasis in this organ. In order to investigate whether the phenotype of *mot1.3-1* plants is caused by a shortage in molybdenum supply, these plants were watered with a nutrient solution containing 5 µg/L ammonium heptamolybdate. Under molybdenum sufficient conditions, *mot1.3-1* mutants exhibited a growth rate, biomass and nitrogenase activity comparable to wild-type plants (Supplemental Figure 9A-9E). A similar result was obtained in hydroponics, a growth condition where molybdenum concentrations can be better controlled (Supplemental Figure 10A-10D). Interestingly, no MOT1 family member was more highly expressed in *mot1.3-1* nodules than in wild-type plants (Supplemental Figure 11).

To validate that the phenotype observed was the result of the *Tnt1* insertion in *MtMOT1.3*, *mot1.3-1* plants were transformed with *MtMOT1.3-HA* construct under its own promoter (same genetic construct used for MtMOT1.3 immunolocalization assay). Insertion of the mutated gene in the *mot1.3-1* mutant under low molybdenum conditions also restored wild-type growth (Figure 5A to 5E), supporting that mutation of *MtMOT1.3* is responsible for this abnormal phenotype. In addition, it also validates the immunofluorescence data, since without a wild type-like expression profile and localization, no complementation would have been observed.

To check whether the lack of MtMOT1.3 activity could affect other processes in the plant, the phenotype of *mot1.3-1* mutant was assayed under non-symbiotic conditions, with

bioRxiv preprint doi: https://doi.org/10.1101/102517; this version posted January 24, 2017. The copyright holder for this preprint (which was not certified by peer review) is the author/funder, who has granted bioRxiv a license to display the preprint in perpetuity. It is made available under aCC-BY-NC-ND 4.0 International license.

nitrate as nitrogen source. In this situation, plant growth relies on the activity of the molybdo-enzyme nitrate reductase to reduce nitrate to nitrite that will be subsequently converted to ammonia and incorporated to amino acids by the glutamine synthetase/glutamine synthase pathway (Bernard and Habash, 2009). In these conditions *mot1.3-1* plants showed a phenotype similar to wild-type plants in terms of growth rate, biomass and nitrate reductase activity, regardless of the Mo availability (Figure 6A to 6C). Therefore, the function of MtMOT1.3 seems to be restricted to symbiotic conditions when symbiotic nitrogen fixation has an important role in plant growth.

Discussion

Obtaining nitrogen from the atmosphere by biological nitrogen fixation is a sustainable alternative to the intensive use of synthetic nitrogen fertilizers in agriculture (Smil, 1999). Legumes are able to use atmospheric N_2 as nitrogen source by means of a symbiotic association with nitrogen-fixing bacteria from the soil, and they occupy between 12 and 15 % of the world arable land (Graham and Vance, 2003). However, maintaining an adequate nitrogen fixation rate involves a complex biological process that requires an efficient nutrient supply from the plant to the rhizobia (Udvardi and Poole, 2013). Molybdenum supply is critical for symbiotic nitrogen fixation since this oligonutrient is needed to synthesize the enzyme nitrogenase, directly involved in the reduction of N_2 to produce NH_4^+. In plants molybdenum is also present in other enzymes carrying out important metabolic processes such as nitrate assimilation (nitrate reductase) or phytohormone biosynthesis (aldehyde oxidase) (Tejada-Jimenez et al., 2013). Little is known about how plants take up molybdate from the soil and redistribute it to the sink organs, although members of the molybdate transport protein family MOT1 are very likely involved in this process in Arabidopsis (Tomatsu et al., 2007; Baxter et al., 2008; Gasber et al., 2011). However, their physiological role in molybdenum homeostasis is still not clear. Less is known for molybdate nutrition in legumes, in spite of the importance of molybdenum in symbiotic nitrogen fixation. Considering the renewed interest and recent advances towards introducing nitrogen fixing abilities into non-legumes (Charpentier and Oldroyd, 2010; Curatti and Rubio, 2014; Lopez-Torrejon et al., 2016) and the need for a more sustainable agriculture (Foley et al., 2011), this gap of our knowledge needs to be

bioRxiv preprint doi: https://doi.org/10.1101/102517; this version posted January 24, 2017. The copyright holder for this preprint (which was not certified by peer review) is the author/funder, who has granted bioRxiv a license to display the preprint in perpetuity. It is made available under aCC-BY-NC-ND 4.0 International license.

filled if we are to ensure proper delivery of molybdenum to produce functional nitrogenase in these new biological systems. Within this context, the present work represents a first but decisive step toward optimization of molybdate allocation for nitrogen fixation, where we have identified a nodule-specific MOT1 member in *M. truncatula* (MtMOT1.3) as responsible for molybdenum supply for symbiotic nitrogen fixation.

Legumes appear to have expanded the number of genes encoding MOT1 proteins in their genome in order to adapt to the presence of an additional molybdenum sink, the root nodule, doubling the average copy number in monocots and other dicots. This is in contrast to genes encoding Nramp transporters, some of which play an essential role in iron transport in rhizobia-infected cells (Kaiser et al., 2003; Tejada-Jimenez et al., 2015), where no significant increase in gene copy numbers were observed. One possible explanation for this, based on the fact that few plant proteins use molybdenum-based cofactors, is that MOT1 transporters are only expressed in very few cell types, highly specialized in the physiological processes catalyzed by Moco or FeMoco-dependent enzymes. If this hypothesis is right, nodule cells should express a specific MOT1 transporter responsible for ensuring molybdenum supply for symbiotic nitrogen fixation, as is the case for *MtMOT1.3* in *M. truncatula.*

Within the nodule, *MtMOT1.3* is expressed in the interzone as well as in the early fixation zone, an expression pattern that is also validated by the transcriptomic data obtained from the Symbimics database (Roux et al., 2014). This expression profile is consistent with a situation in which the rhizobia-infected cell is increasing its molybdenum content to transfer it to the bacteroids, so that when the physiological conditions are right, they can start synthesizing FeMoco. In contrast, iron-transporting *MtNramp1*, responsible for iron uptake by rhizobia-infected cells, shows a different expression profile, with a maximum of expression in the infection/differentiation zone (Tejada-Jimenez et al., 2015). This difference for the expression of iron and molybdenum transporter genes indicates that the uptake of these two elements occurs in two separate moments during nodule development, probably reflecting an earlier need for certain ferroproteins other than nitrogenase. It also indicates that molybdate release from the vasculature for uptake by rhizobia-infected cells occurs at the interzone and early fixation zone, in contrast to what has been proposed for iron and other transition metals (Rodriguez-Haas et al., 2013;

bioRxiv preprint doi: https://doi.org/10.1101/102517; this version posted January 24, 2017. The copyright holder for this preprint (which was not certified by peer review) is the author/funder, who has granted bioRxiv a license to display the preprint in perpetuity. It is made available under aCC-BY-NC-ND 4.0 International license.

González-Guerrero et al., 2014; Tejada-Jimenez et al., 2015; González-Guerrero et al., 2016). However, neither *MtMOT1.3* nor *MtNramp1* are expressed in the older parts of the fixation zone. This suggests that no additional metal uptake is taking place in this zone, indicating either a high degree of protein stability in the fixation zone, or an effective recycling of essential metallic nutrients.

MtMOT1.3 is a plasma membrane-bound protein, as indicated by both the immunolocalization of a HA-tagged fusion in *M. truncatula* nodules and the colocalization studies of MtMOT1-GFP with a plasma membrane marker in tobacco leaves. In Arabidopsis, while AtMOT1.2 is clearly localized in the vacuole of leaf cells (Gasber et al., 2011), contradicting localization data have been reported for AtMOT1.1, claiming either plasma membrane or mitochondrial localizations (Tomatsu et al., 2007; Baxter et al., 2008). These conflicting data seem to be caused by the GFP marker fused to AtMOT1.1, since when it is fused to the N-terminus of AtMOT1.1 it leads to plasma membrane localization, while the C-terminus fusion results in mitochondrial localization. Our MtMOT1.3 subcellular localization data have been obtained using two different methodologies: immunolocalization in *M. truncatula* cells by detecting HA epitope fused to MtMOT1.3 and transient expression in *N. benthamiana* fused to GFP. Both approaches yielded the same result reinforcing MtMOT1.3 localization in the plasma membrane. Furthermore, expressing *MtMOT1.3-HA* in a *mot1.3-1* mutant background resulted in a complementation of the wild-type phenotype, which indicates that the expressed transporter is being targeted to the proper subcellular compartment.

Like other members of the MOT1 family, MtMOT1.3 transports molybdate towards the cytosol, as indicated by the yeast toxicity assays. The phenotype characterization of a *Tnt1* mutant line strongly suggests that this activity is used by *M. truncatula* to introduce molybdate into nodule cells. The knockout mutant line *mot1.3-1* has lower nitrogenase activity than wild-type control plants. Consequently, plant growth is reduced due to lack of fixed nitrogen. Nodules from *mot1.3-1* are on average smaller than those from wild-type plants. This does not seem to be caused by a delayed nodulation, since nodulation kinetics are very similar to wild-type plants. Neither it is due to an alteration of the nodulation process, as the nodule organization does not show any alteration in *mot1.3-1* nodules. Alternatively, it could be hypothesized that the cause is the reduced uptake of a nutrient

bioRxiv preprint doi: https://doi.org/10.1101/102517; this version posted January 24, 2017. The copyright holder for this preprint (which was not certified by peer review) is the author/funder, who has granted bioRxiv a license to display the preprint in perpetuity. It is made available under aCC-BY-NC-ND 4.0 International license.

essential for nodule functioning. The *mot1.3-1* phenotype is molybdenum-dependent, since molybdate fortification of the nutritive solution resulted in wild-type looking *mot1.3-1* plants, in apparent contradiction to the higher levels of molybdenum detected in *mot1.3-1* nodules. This accumulation pattern has also been observed when studying a nodule-specific plasma membrane copper transporter and a nodule-induced plasma membrane zinc transporter (unpublished data). One possible explanation is the existence of a signal indicating intracellular metal deficiency that would trigger more metal being transported to the nodule. Since the uptake transporter is not present, this would result in metal accumulation in the nodule apoplast and in the vasculature. This phenotype reversal by increasing the molybdate content of the nutritive solution is likely the result of other membrane transporters that at higher molybdate concentration could counterbalance the absence of MtMOT1.3 activity. In *M. truncatula* all the MOT1 proteins have shown expression within the nodule, although only *MtMOT1.3* exhibited a nodule-specific transcription pattern. It could be argued that either MtMOT1.2, MtMOT1.4, or MtMOT1.5 could carry out this role. If this were the case, an induction of its expression levels in *mot1.3-1* nodules would be expected. However, we observe a slight reduction of their expression levels, suggesting a different role in molybdenum homeostasis in nodules. Alternatively, sulfate transporters could also compensate the lack of MtMOT1.3; for instance, the sulfate transporter SHST1 from the legume *Stylosanthes hamata* is able to transport molybdate upon expression in *Saccharomyces cerevisiae* (Fitzpatrick et al., 2008). Furthermore, proteins of the MOT2 family have been also related to molybdate transport in the green alga *C. reinhardtii* (Tejada-Jimenez et al., 2011) and members of the MOT2 family are present in *M. truncatula* genome. However according to the transcriptomic database Symbimics, none of SHST1 or MOT2 orthologues in *M. truncatula* are significantly expressed in nodules (Roux et al., 2014), which indicates that either another MOT1 transporter carried out this role in spite of the reduced expression levels, or a member of a yet-to-be-identified molybdate transporter family would be supplementing MtMOT1.3 function.

Under non-symbiotic conditions, MtMOT1.3 does not play an essential role, as indicated by its expression profile and by the lack of phenotype observed under these conditions. Even when the plants require Moco-dependent nitrate reductase activity to

bioRxiv preprint doi: https://doi.org/10.1101/102517; this version posted January 24, 2017. The copyright holder for this preprint (which was not certified by peer review) is the author/funder, who has granted bioRxiv a license to display the preprint in perpetuity. It is made available under aCC-BY-NC-ND 4.0 International license.

grow, no differences were observed between mutant and wild-type plants. These results reinforce the hypothesis of specialization of a legume MOT1 transporter during evolution to provide molybdenum for symbiotic nitrogen fixation.

In conclusion, molybdate transported by the host plant is released from the vasculature into the apoplast of the interzone/early fixation zone (Figure 7). From there, MtMOT1.3 is responsible for introducing molybdate into rhizobia infected cells, as well as in the non-infected ones. The latter raises the question of why the non-infected cells would require molybdenum. Possible explanations would be that they are being prepared if they become infected, that they are buffering or storing molybdenum to be used later, or that this molybdenum is required to synthesize active Moco-dependent enzymes in these cells. Once in the cell cytosol, molybdate has to be transported across the symbiosome membrane. Since no molybdate-specific efflux system is known, it could be speculated that this role is carried out by a sulfate transporter specific of this membrane such as SST1, whose mutation has a severe impact on nitrogenase activity (Krusell et al., 2005). Once in the peribacteroid space, ModABC would introduce molybdate into the bacteroid (Delgado et al., 2006; Cheng et al., 2016).

Methods

Biological material and growth conditions

M. truncatula R108 seeds were scarified in the presence of concentrated sulfuric acid for 7 min. Then, seeds were washed several times with cold water, surface sterilized with 50 % (v/v) bleach for 90 s and incubated overnight with sterile water in the dark. After 48 h at 4 ºC, seeds were germinated in water-agar plates 0.8 % (w/v). Seedlings were transferred to sterile perlite pots or to Jenner's solution for hydroponic growth (Brito et al., 1994), and inoculated with *S. meliloti* 2011 or the same bacterial strain transformed pHC60 (Cheng and Walker, 1998). Plants were grown in a greenhouse under 16 h light and 22 ºC. In the case of perlite pots, plants were watered every two days with Jenner's solution or water alternatively. Nodules were collected 28 dpi. Plants growing under non-symbiotic conditions were supplemented every two weeks with 2 mM KNO_3. *Agrobacterium rhizogenes* strain ARqua1 having the appropriate vector was used for *M. truncatula* hairy-root transformation (Boisson-Dernier et al., 2001). Agroinfiltration for transitory expression

bioRxiv preprint doi: https://doi.org/10.1101/102517; this version posted January 24, 2017. The copyright holder for this preprint (which was not certified by peer review) is the author/funder, who has granted bioRxiv a license to display the preprint in perpetuity. It is made available under aCC-BY-NC-ND 4.0 International license.

experiments were performed in *N. benthamiana* leaves using *A. tumefaciens* C58C1 carrying the corresponding genetic construct.

S. cerevisiae strain 31019b (MATa *ura3 mep1Δ mep2Δ::LEU2 mep3Δ:: KanMX2*) was used for heterologous expression assays (Marini et al., 1997). Yeasts were grown in synthetic dextrose (SD) or yeast peptone dextrose medium supplemented with 2 % glucose (Sherman et al., 1986).

Quantitative real-time RT-PCR

Transcriptional expression studies were carried out by real-time RT-PCR (StepOne plus, Applied Biosystems) using the Power SyBR Green master mix (Applied Biosystems). Primers used are indicated in Supplemental Table 2. RNA levels were normalized by using the *ubiquitin carboxy-terminal hydrolase* gene as internal standard. RNA isolation and cDNA synthesis were carried out as previously described (Tejada-Jimenez et al., 2015).

GUS Staining

pMtMOT1.3::GUS construct was obtained by amplifying 1.1 kb upstream of the *MtMOT1.3* (Nakagawa et al., 2007) start codon using the primers 5MtMOT1.3pGW and 3MtMOT1.3pGW (Supplemental Table 2). The resulting fragment was cloned by Gateway cloning technology (Invitrogen) into pGWB3 vector. Hairy-root transformation was carried out as described above. GUS staining was performed in root of 28-dpi plants as previously described (Vernoud et al., 1999). Nodules sections were clarified with 50% bleach for 30 min.

Immunohistochemistry and confocal microscopy

A genomic region comprising *MtMOT1.3* full gene and 1.1 kb upstream of its start codon was cloned into pGWB13 vector (Nakagawa et al., 2007) using Gateway cloning technology (Invitrogen). The resulting genetic construct contains *MtMOT1.3* gene under the control of its own promoter and with three C-terminal HA epitopes in frame. Hairy-root transformation was carried out as indicated above. *M. truncatula* transformed plants were inoculated with *S. meliloti* 2011 constitutively expressing GFP. Nodules and roots were collected at 28-dpi and fixed at 4 ºC overnight in 4 % (w/v) paraformaldehyde and 2.5 %

bioRxiv preprint doi: https://doi.org/10.1101/102517; this version posted January 24, 2017. The copyright holder for this preprint (which was not certified by peer review) is the author/funder, who has granted bioRxiv a license to display the preprint in perpetuity. It is made available under aCC-BY-NC-ND 4.0 International license.

(w/v) sucrose in phosphate-buffered saline (PBS). Fixed plant material was sectioned, 100 µm wide, with a Vibratome 1000 Plus. Sections were dehydrated by serial incubation with methanol (30 %, 50 %, 70 % and 100 % [v/v] in PBS) for 5 min and then rehydrated following the same methanol series in reverse order. Cell wall permeabilization was carried out by incubation with 2 % (w/v) cellulase in PBS for 1 h and 0.1 % (v/v) Tween 20 for 15 min. Sections were blocked with 5 % (w/v) bovine serum albumin in PBS and then incubated with 1:50 anti-HA mouse monoclonal antibody (Sigma) in PBS at room temperature for 2 h. Primary antibody was washed three times with PBS for 10 min and subsequently incubated with 1:40 Alexa594-conjugated anti-mouse rabbit monoclonal antibody (Sigma) in PBS at room temperature for 1 h. Secondary antibody was washed three times with PBS for 10 min, and then DNA was stained using DAPI. Images were obtained with a confocal laser-scanning microscope (Leica SP8).

Transient expression in *N. benthamiana* leaves

MtMOT1.3 transient expression in tobacco leaves was carried out as previously described (Voinnet et al., 2003). *MtMOT1.3* CDS was cloned into pGWB5 (Nakagawa et al., 2007) by Gateway cloning technology (Invitrogen), resulting in C-terminal fusion to GFP. *A. tumefaciens* C58C1 (Deblaere et al., 1985) cells independently transformed with this construct, with the plasma membrane marker pm-CFP pBIN (Nelson et al., 2007) or with the silencing suppressor p19 of *Tomato bushy stunt virus* (Voinnet et al., 2003) were injected into 4-week-old *N. benthamiana* leaves. Expression of the appropriate construct was analyzed after 3 d by confocal laser-scanning microscopy (Leica).

Nitrogenase activity

Acetylene reduction assay was used to measure nitrogenase activity (Hardy et al., 1968). Wild-type and mutant plants 28 dpi were separately introduced in 30-mL tubes. Each tube was sealed with rubber stoppers and contained five independently transformed plants. Three mililiters of air of each bottle was replaced by the same volume of acetylene, tubes were subsequently incubated for 30 min at room temperature. Produced ethylene was measured by analyzing 0.5 mL of gas from each bottle in a Shimadzu GC-8A gas chromatograph using a Porapak N column.

bioRxiv preprint doi: https://doi.org/10.1101/102517; this version posted January 24, 2017. The copyright holder for this preprint (which was not certified by peer review) is the author/funder, who has granted bioRxiv a license to display the preprint in perpetuity. It is made available under aCC-BY-NC-ND 4.0 International license.

Metal content determination

Inductively coupled plasma optical emission spectrometry was carried out at the Unit of Metal Analysis in the Scientific and Technology Centres of the Universidad de Barcelona (Spain).

Nitrate reductase activity

Nitrate reductase activity was analyzed as described by Scheible et al. (Scheible et al., 1997) with some modifications. We started from 100 mg of fresh leaves. The extraction buffer used for crude extracts preparation contained 100 mM potassium phosphate pH 7.5, 5 mM magnesium acetate, 10 % glycerol (v/v), 10 % polyvinylpolypyrrolidone (w/v), 0.1 % Triton X-100, 1 mM EDTA, 0.05 % ß-mercaptoethanol, 1 mM PMSF. Plant material was homogenized with liquid nitrogen and 1:6 extraction buffer (v/v). The crude extract was centrifuged at 14,000 x*g* at 4 ºC for 15 min. The reaction was initiated by adding 0.05 mL of crude extract to 0.5 mL of reaction buffer and incubated at 30 ºC for 20 min. The reaction buffer contained 50 mM potassium phosphate pH 7.5, 10 mM KNO_3, 5 mM EDTA and 0.5 mM NADH. Nitrate reduction reaction was stopped by adding 1 volume of 1 % sulfanilamide in 2.4 M HCl, and 1 volume of 0.02 % N-1-naphtyl-ethylenediamine. After centrifugation absorbance at 540 nm was measured in UV/visible spectrophotometer Ultrospect 3300 pro (Amersham Bioscience).

Bioinformatics

Members of the MOT1 family in *M. truncatula* were identified by the Basic Local Alignment Search Tool in the *M. truncatula* Genome Project database (http://www.jcvi.org/medicago/index.php), using as reference sequence a member of the MOT1 family from Arabidopsis (NP_180139). Protein sequence alignment and unrooted tree visualization were performed with MEGA7 package (http://www.megasoftware.net/) using ClustalW software and neighbor joining algorithm. Accession numbers: *Arabidopsis thaliana* AtMOT1.1, NP_180139.1; AtMOT1.2, NP_178147.1; AtSULTR1.1, NP_192602.1; AtSULTR2.1, NP_196580.1; AtSULTR3.1, ANM64117.1; AtSULTR4.1, AED91910.1; *Brassica napus* BnMOT1.1, XP_013709878.1; BnMOT1.3,

bioRxiv preprint doi: https://doi.org/10.1101/102517; this version posted January 24, 2017. The copyright holder for this preprint (which was not certified by peer review) is the author/funder, who has granted bioRxiv a license to display the preprint in perpetuity. It is made available under aCC-BY-NC-ND 4.0 International license.

XP_013667816.1; BnSULTR1.1, XP_013715602.1; BnSULTR2.1, NP_001302517.1; BnSULTR3.1, XP_013737126.1; BnSULTR4.1, XP_013667920.1; *Glycine max* GmMOT1.1, XP_003545516.1; GmMOT1.4, KRH05029.1; GmMOT1.6, XP_003527804.1; GmMOT1.7, XP_003523708.1; GmSULTR1.3, XP_006593569.1; GmSULTR2.1, XP_003531538.1; GmSULTR3.1, XP_003521258.1; GmSULTR4.2, XP_003552670.1; *Lotus japonicus* LjMOT1.1, AFK43331.1; LjMOT1.2, AJE26312.1; LjSST1, CAL36108.1; *Medicago truncatula* MtMOT1.1, XP_013465770.1; MtMOT1.2, XP_013465776.1; MtMOT1.3, XP_013460259.1; MtMOT1.4, XP_013454709.1; MtMOT1.5, XP_003603486.1; MtSULTR1.1, XP_003614968.1; MtSAT1, XP_003602002.1; *Oryza sativa* OsMOT1.1, XP_015650610.1; OsMOT1.2, XP_015621613.1; OsSULTR1.2 XP_015650733.1; OsSULTR2.1, ABF94445.1; OsSULTR3.1, BAS82415.1; OsSULTR4.1, XP_015612472.1; *Phaseolus vulgaris* PvMOT1.1, XP_007161270.1; PvMOT1.2, XP_007137089.1; PvMOT1.3, XP_007161272.1; PvMOT1.4, XP_007135722.1; PvSULTR1.1, XP_007141140.1; PvSULTR2.1, XP_007163633.1; PvSULTR3.1, XP_007162459.1; PvSULTR4.1, XP_007139276.1; *Vitis vinifera* VvMOT1.1, XP_002281989.2; VvMOT1.2, XP_002285217.1; VvSULTR1.1, XP_010664070.1; VvSULTR2.1, XP_010652824.1; VvSULTR3.1, XP_003632327.1; VvSULTR4.2, XP_002282491.2.

Statistical tests

Data were analyzed by Student's unpaired t test to calculate statistical significance of observed differences. Test results with p-values less than 0.05 were considered as statistically significant.

bioRxiv preprint doi: https://doi.org/10.1101/102517; this version posted January 24, 2017. The copyright holder for this preprint (which was not certified by peer review) is the author/funder, who has granted bioRxiv a license to display the preprint in perpetuity. It is made available under aCC-BY-NC-ND 4.0 International license.

Acknowledgments

This research was funded by a European Research Council Starting Grant (ERC-2013-StG-335284), to MGG. Development of *M. truncatula Tnt1* mutant population was, in part, funded by the National Science Foundation, USA (DBI-0703285) to KSM. We would also like to acknowledge the other members of laboratory 281 at Centro de Biotecnología y Genómica de Plantas (UPM-INIA) for their support and feedback in preparing this manuscript.

Author contribution

MTJ carried out most of the experiments. PGD performed the confocal microscopy using the anti-HA Alexa488-conjugated antibody, the nodule development cross-section, and the molybdenum content in nodules. JLM carried out the expression of MOT1 genes in the *mot1.3-1* mutant, as well as studied the effecto of molybdate concentrations in transcription levels. Both PGD and JLM studied the nodulation process in wild type and *mot1.3-1* plants over time. JW and KSM performed *Medicago truncatula* mutant screening and isolated the *mot1.3-1* allele. MTJ, JI, and MGG designed the experiments, analyzed the data and wrote the article.

bioRxiv preprint doi: https://doi.org/10.1101/102517; this version posted January 24, 2017. The copyright holder for this preprint (which was not certified by peer review) is the author/funder, who has granted bioRxiv a license to display the preprint in perpetuity. It is made available under aCC-BY-NC-ND 4.0 International license.

References

Baxter, I., Muthukumar, B., Park, H.C., Buchner, P., Lahner, B., Danku, J., Zhao, K., Lee, J., Hawkesford, M.J., Guerinot, M.L., and Salt, D.E. (2008). Variation in molybdenum content across broadly distributed populations of *Arabidopsis thaliana* is controlled by a mitochondrial molybdenum transporter (MOT1). PLoS Genet **4,** e1000004.

Bernard, S.M., and Habash, D.Z. (2009). The importance of cytosolic glutamine synthetase in nitrogen assimilation and recycling. New Phytol **182,** 608-620.

Boisson-Dernier, A., Chabaud, M., Garcia, F., Becard, G., Rosenberg, C., and Barker, D.G. (2001). *Agrobacterium rhizogenes*-transformed roots of *Medicago truncatula* for the study of nitrogen-fixing and endomycorrhizal symbiotic associations. Mol Plant Microbe Interact **14,** 695-700.

Brewin, N.J. (1991). Development of the legume root nodule. Annu Rev Cell Biol **7,** 191-226.

Brito, B., Palacios, J.M., Hidalgo, E., Imperial, J., and Ruiz-Argueso, T. (1994). Nickel availability to pea (*Pisum sativum* L.) plants limits hydrogenase activity of *Rhizobium leguminosarum* bv. *viciae* bacteroids by affecting the processing of the hydrogenase structural subunits. J Bacteriol **176,** 5297-5303.

Charpentier, M., and Oldroyd, G. (2010). How close are we to nitrogen-fixing cereals? Curr Opin Plant Biol **13,** 556-564.

Cheng, G., Karunakaran, R., East, A.K., and Poole, P.S. (2016). Multiplicity of sulfate and molybdate transporters and their role in nitrogen fixation in *Rhizobium leguminosarum* bv. *viciae* Rlv3841. Mol Plant Microbe Interact **29,** 143-152.

Cheng, H.P., and Walker, G.C. (1998). Succinoglycan is required for initiation and elongation of infection threads during nodulation of alfalfa by *Rhizobium meliloti.* J Bacteriol **180,** 5183-5191.

Cheng, X., Wen, J., Tadege, M., Ratet, P., and Mysore, K.S. (2011). Reverse genetics in *Medicago truncatula* using *Tnt1 i*nsertion mutants. Methods Mol Biol **678,** 179-190.

Cheng, X., Wang, M., Lee, H.K., Tadege, M., Ratet, P., Udvardi, M., Mysore, K.S., and Wen, J. (2014). An efficient reverse genetics platform in the model legume *Medicago truncatula*. New Phytol **201,** 1065-1076.

bioRxiv preprint doi: https://doi.org/10.1101/102517; this version posted January 24, 2017. The copyright holder for this preprint (which was not certified by peer review) is the author/funder, who has granted bioRxiv a license to display the preprint in perpetuity. It is made available under aCC-BY-NC-ND 4.0 International license.

Curatti, L., and Rubio, L.M. (2014). Challenges to develop nitrogen-fixing cereals by direct nif-gene transfer. Plant Sci **225,** 130-137.

Deblaere, R., Bytebier, B., De Greve, H., Deboeck, F., Schell, J., Van Montagu, M., and Leemans, J. (1985). Efficient octopine Ti plasmid-derived vectors for Agrobacterium-mediated gene transfer to plants. Nucleic Acids Res **13,** 4777-4788.

Delgado, M.J., Tresierra-Ayala, A., Talbi, C., and Bedmar, E.J. (2006). Functional characterization of the *Bradyrhizobium japonicum modA* and *modB* genes involved in molybdenum transport. Microbiology **152,** 199-207.

Dilworth, M.J. (1966). Acetylene reduction by nitrogen-fixing preparations from *Clostridium pasteurianum*. Biochim Biophys Acta **127,** 285-294.

Esteifel, E.I. (2002). Molybdenum and tungsten: their roles in biological processes. In Metal ions in biological systems, A. Sigel and H. Sigel, eds (New York: Marcel Dekker Inc.), pp. 1-30.

Fitzpatrick, K.L., Tyerman, S.D., and Kaiser, B.N. (2008). Molybdate transport through the plant sulfate transporter SHST1. FEBS Lett **582,** 1508-1513.

Foley, J.A., Ramankutty, N., Brauman, K.A., Cassidy, E.S., Gerber, J.S., Johnston, M., Mueller, N.D., O'Connell, C., Ray, D.K., West, P.C., Balzer, C., Bennett, E.M., Carpenter, S.R., Hill, J., Monfreda, C., Polasky, S., Rockstrom, J., Sheehan, J., Siebert, S., Tilman, D., and Zaks, D.P. (2011). Solutions for a cultivated planet. Nature **478,** 337-342.

Gao, J.S., Wu, F.F., Shen, S.L., Meng, Y., Cai, Y.P., and Lin, Y. (2016). A putative molybdate transporter LjMOT1 is required for molybdenum transport in *Lotus japonicus*. Physiol. Plant. **158**, 331-340.

Gasber, A., Klaumann, S., Trentmann, O., Trampczynska, A., Clemens, S., Schneider, S., Sauer, N., Feifer, I., Bittner, F., Mendel, R.R., and Neuhaus, H.E. (2011). Identification of an Arabidopsis solute carrier critical for intracellular transport and inter-organ allocation of molybdate. Plant Biol (Stuttg) **13,** 710-718.

Georgiadis, M.M., Komiya, H., Chakrabarti, P., Woo, D., Kornuc, J.J., and Rees, D.C. (1992). Crystallographic structure of the nitrogenase iron protein from *Azotobacter vinelandii*. Science **257,** 1653-1659.

bioRxiv preprint doi: https://doi.org/10.1101/102517; this version posted January 24, 2017. The copyright holder for this preprint (which was not certified by peer review) is the author/funder, who has granted bioRxiv a license to display the preprint in perpetuity. It is made available under aCC-BY-NC-ND 4.0 International license.

González-Guerrero, M., Matthiadis, A., Saez, A., and Long, T.A. (2014). Fixating on metals: new insights into the role of metals in nodulation and symbiotic nitrogen fixation. Front Plant Sci **5,** 45.

González-Guerrero, M., Escudero, V., Saez, A., and Tejada-Jimenez, M. (2016). Transition metal transport in plants and associated endosymbionts: Arbuscular mycorrhizal fungi and rhizobia. Front Plant Sci **7,** 1088.

Graham, P.H., and Vance, C.P. (2003). Legumes: importance and constraints to greater use. Plant Physiol **131,** 872-877.

Hardy, R.W., Holsten, R.D., Jackson, E.K., and Burns, R.C. (1968). The acetylene-ethylene assay for n(2) fixation: laboratory and field evaluation. Plant Physiol **43,** 1185-1207.

Hernandez, J.A., George, S.J., and Rubio, L.M. (2009). Molybdenum trafficking for nitrogen fixation. Biochemistry **48,** 9711-9721.

Kaiser, B.N., Gridley, K.L., Ngaire Brady, J., Phillips, T., and Tyerman, S.D. (2005). The role of molybdenum in agricultural plant production. Ann Bot **96,** 745-754.

Kaiser, B.N., Moreau, S., Castelli, J., Thomson, R., Lambert, A., Bogliolo, S., Puppo, A., and Day, D.A. (2003). The soybean NRAMP homologue, GmDMT1, is a symbiotic divalent metal transporter capable of ferrous iron transport. Plant J **35,** 295-304.

Kondorosi, E., Banfalvi, Z., and Kondorosi, A. (1984). Physical and genetic analysis of a symbiotic region of *Rhizobium meliloti*: identification of nodulation genes. Mol Gen Genet **193,** 445-452.

Krusell, L., Krause, K., Ott, T., Desbrosses, G., Kramer, U., Sato, S., Nakamura, Y., Tabata, S., James, E.K., Sandal, N., Stougaard, J., Kawaguchi, M., Miyamoto, A., Suganuma, N., and Udvardi, M.K. (2005). The sulfate transporter SST1 is crucial for symbiotic nitrogen fixation in *Lotus japonicus* root nodules. Plant Cell **17,** 1625-1636.

Lopez-Torrejon, G., Jimenez-Vicente, E., Buesa, J.M., Hernandez, J.A., Verma, H.K., and Rubio, L.M. (2016). Expression of a functional oxygen-labile nitrogenase component in the mitochondrial matrix of aerobically grown yeast. Nat Commun **7,** 11426.

bioRxiv preprint doi: https://doi.org/10.1101/102517; this version posted January 24, 2017. The copyright holder for this preprint (which was not certified by peer review) is the author/funder, who has granted bioRxiv a license to display the preprint in perpetuity. It is made available under aCC-BY-NC-ND 4.0 International license.

Marini, A.M., Soussi-Boudekou, S., Vissers, S., and Andre, B. (1997). A family of ammonium transporters in *Saccharomyces cerevisiae*. Mol Cell Biol **17,** 4282-4293.

Maupin-Furlow, J.A., Rosentel, J.K., Lee, J.H., Deppenmeier, U., Gunsalus, R.P., and Shanmugam, K.T. (1995). Genetic analysis of the *modABCD* (molybdate transport) operon of *Escherichia coli*. J Bacteriol **177,** 4851-4856.

Mendel, R.R., and Hansch, R. (2002). Molybdoenzymes and molybdenum cofactor in plants. J Exp Bot **53,** 1689-1698.

Mendel, R.R., and Bittner, F. (2006). Cell biology of molybdenum. Biochim Biophys Acta **1763,** 621-635.

Nakagawa, T., Kurose, T., Hino, T., Tanaka, K., Kawamukai, M., Niwa, Y., Toyooka, K., Matsuoka, K., Jinbo, T., and Kimura, T. (2007). Development of series of gateway binary vectors, pGWBs, for realizing efficient construction of fusion genes for plant transformation. J Biosci Bioeng **104,** 34-41.

Nelson, B.K., Cai, X., and Nebenfuhr, A. (2007). A multicolored set of in vivo organelle markers for co-localization studies in Arabidopsis and other plants. Plant J **51,** 1126-1136.

Oldroyd, G.E. (2013). Speak, friend, and enter: signalling systems that promote beneficial symbiotic associations in plants. Nat Rev Microbiol **11,** 252-263.

Rodriguez-Haas, B., Finney, L., Vogt, S., González-Melendi, P., Imperial, J., and González-Guerrero, M. (2013). Iron distribution through the developmental stages of *Medicago truncatula* nodules. Metallomics **5,** 1247-1253.

Roux, B., Rodde, N., Jardinaud, M.F., Timmers, T., Sauviac, L., Cottret, L., Carrere, S., Sallet, E., Courcelle, E., Moreau, S., Debelle, F., Capela, D., de Carvalho-Niebel, F., Gouzy, J., Bruand, C., and Gamas, P. (2014). An integrated analysis of plant and bacterial gene expression in symbiotic root nodules using laser-capture microdissection coupled to RNA sequencing. Plant J **77,** 817-837.

Rubio, L.M., and Ludden, P.W. (2008). Biosynthesis of the iron-molybdenum cofactor of nitrogenase. Annu Rev Microbiol **62,** 93-111.

Scheible, W.R., Gonzalez-Fontes, A., Morcuende, R., Lauerer, M., Geiger, M., Glaab, J., Gojon, A., Schulze, E.D., and Stitt, M. (1997). Tobacco mutants with a decreased number of functional nia genes compensate by modifying the diurnal

bioRxiv preprint doi: https://doi.org/10.1101/102517; this version posted January 24, 2017. The copyright holder for this preprint (which was not certified by peer review) is the author/funder, who has granted bioRxiv a license to display the preprint in perpetuity. It is made available under aCC-BY-NC-ND 4.0 International license.

regulation of transcription, post-translational modification and turnover of nitrate reductase. Planta **203,** 304-319.

Schöllhorn, R., and Burris, R.H. (1966). Study of intermediates in nitrogen fixation. Fed Proc **25,** 710.

Sherman, F., Fink, G.R., and Hicks, J.B. (1986). Methods in yeast genetics. (Plainview, NY: Cold Spring Harbor Lab Press).

Smil, V. (1999). Nitrogen in crop production: An account of global flows. Global biogeochemical cycles **13,** 647-662.

Smith, F.W., Ealing, P.M., Hawkesford, M.J., and Clarkson, D.T. (1995). Plant members of a family of sulfate transporters reveal functional subtypes. Proc Natl Acad Sci U S A **92,** 9373-9377.

Sprent, J.I. (2007). Evolving ideas of legume evolution and diversity: a taxonomic perspective on the occurrence of nodulation. New Phytol **174,** 11-25.

Stout, P.R., Meagher, W.R., Pearson, G.A., and Johnson, C.M. (1951). Molybdenum nutrition of crop plants: I. The influence of phosphate and sulfate on the absortion of molybdenum from soils and solution cultures. Plant and Soil **3,** 51-87.

Tadege, M., Wen, J., He, J., Tu, H., Kwak, Y., Eschstruth, A., Cayrel, A., Endre, G., Zhao, P.X., Chabaud, M., Ratet, P., and Mysore, K.S. (2008). Large-scale insertional mutagenesis using the Tnt1 retrotransposon in the model legume *Medicago truncatula*. Plant J **54,** 335-347.

Tejada-Jimenez, M., Galvan, A., and Fernandez, E. (2011). Algae and humans share a molybdate transporter. Proc Natl Acad Sci U S A **108,** 6420-6425.

Tejada-Jimenez, M., Llamas, A., Sanz-Luque, E., Galvan, A., and Fernandez, E. (2007). A high-affinity molybdate transporter in eukaryotes. Proc Natl Acad Sci U S A **104,** 20126-20130.

Tejada-Jimenez, M., Chamizo-Ampudia, A., Galvan, A., Fernandez, E., and Llamas, A. (2013). Molybdenum metabolism in plants. Metallomics **5,** 1191-1203.

Tejada-Jimenez, M., Castro-Rodriguez, R., Kryvoruchko, I., Lucas, M.M., Udvardi, M., Imperial, J., and González-Guerrero, M. (2015). *Medicago truncatula* natural resistance-associated macrophage Protein1 is required for iron uptake by rhizobia-infected nodule cells. Plant Physiol **168,** 258-272.

bioRxiv preprint doi: https://doi.org/10.1101/102517; this version posted January 24, 2017. The copyright holder for this preprint (which was not certified by peer review) is the author/funder, who has granted bioRxiv a license to display the preprint in perpetuity. It is made available under aCC-BY-NC-ND 4.0 International license.

Tomatsu, H., Takano, J., Takahashi, H., Watanabe-Takahashi, A., Shibagaki, N., and Fujiwara, T. (2007). An *Arabidopsis thaliana* high-affinity molybdate transporter required for efficient uptake of molybdate from soil. Proc Natl Acad Sci U S A **104,** 18807-18812.

Udvardi, M., and Poole, P.S. (2013). Transport and metabolism in legume-rhizobia symbioses. Annu Rev Plant Biol **64,** 781-805.

Vasse, J., de Billy, F., Camut, S., and Truchet, G. (1990). Correlation between ultrastructural differentiation of bacteroids and nitrogen fixation in alfalfa nodules. J Bacteriol **172,** 4295-4306.

Vernoud, V., Journet, E.P., and Barker, D.G. (1999). MtENOD20, a Nod factor-inducible molecular marker for root cortical cell activation. Molecular Plant-Microbe Interactions **12,** 604-614.

Voinnet, O., Rivas, S., Mestre, P., and Baulcombe, D. (2003). An enhanced transient expression system in plants based on suppression of gene silencing by the p19 protein of tomato bushy stunt virus. Plant J **33,** 949-956.

bioRxiv preprint doi: https://doi.org/10.1101/102517; this version posted January 24, 2017. The copyright holder for this preprint (which was not certified by peer review) is the author/funder, who has granted bioRxiv a license to display the preprint in perpetuity. It is made available under aCC-BY-NC-ND 4.0 International license.

Figure Legends

Figure 1. MtMOT1.3 is a member of the MOT1 protein and is expressed in the nodule. (A) Unrooted tree of the plant SULTR and MOT1 families. (B) Alignment of the conserved motifs of the MOT1 proteins present in all *M. truncatula* MOT1 members. Sequences were aligned using ClustalW method and it is extracted from a larger alignment including the full protein sequence of the *M. truncatula* MOT1 members. (C) Determination of *MtMOT1.3* expression in nodulated and nitrogen-fertilized *M. truncatula* plants relative to the internal standard gene Ubiquitin carboxyl-terminal hydrolase. Data are the mean ± SD of two independent experiments with 4 pooled plants. n.d., non-detected. (D) *MtMOT1.3* expression in nodulated and nitrogen-fertilized *M. truncatula* plants. *Ubiquitin carboxyl-terminal hydrolase1* (*MtUb1*) was used as control for PCR amplifications.

Figure 2. MtMOT1.3 transports molybdate towards the cytosol. (A) *S. cerevisiae* strain 31019b was transformed with PDR196 empty vector or PDR196 containing *MtMOT1.3* coding sequence, and grown at 28 ºC for 3d in serial dilution (10X) on SD solid medium medium without an added molybdenum source or containing 50 µM sodium molybdate. (B) *S. cerevisiae* strains used in (A) were grown in SD liquid medium, with and without 50µM sodium molybdate, at 28 ºC for 42 h. Yeast growth was monitored by measuring optical density at 600 nm every 3h. (C) Molybdenum content in the yeast grown in (B) after 42 h. Data are the mean ± SD of two independent experiments.

Figure 3. *MtMOT1.3* gene is expressed in the interzone and fixation zone of *M. truncatula* nodules. (A) and (B) GUS staining of *M. truncatula* 28-dpi nodules transiently expressing *gus* gene under the control of *MtMOT1.3* promoter. (A) Intact nodule. (B) Longitudinal nodule section. Bars = 200 µm. (C) Expression of *MtMOT1.3* in *M. truncatula* nodules by laser-capture microdissection coupled to RNA sequencing. Data were obtained from the Symbimics database (https://iant.toulouse.inra.fr/symbimics/). Meris, meristem; Infec, infection zone; Differ, differentiation zone; Inter, interzone; Fix, fixation zone.

bioRxiv preprint doi: https://doi.org/10.1101/102517; this version posted January 24, 2017. The copyright holder for this preprint (which was not certified by peer review) is the author/funder, who has granted bioRxiv a license to display the preprint in perpetuity. It is made available under aCC-BY-NC-ND 4.0 International license.

Figure 4. MtMOT1.3 is localized in the plasma membrane. (A) to (C) Cross section of a 28-dpi *M. truncatula* nodule transiently expressing MtMOT1.3-HA construct and infected with a *S. meliloti* strain constitutively expressing GFP (green). MtMOT1.3-HA was detected using an Alexa-594-conjugated antibody (red). (A) MtMOT1.3-HA signal. (B) Overlay of MtMOT1.3-HA and *S. meliloti* signals. (C) Overlay of MtMOT1.3-HA signal and differential interference contrast. a, meristem; b, infection/differentiation; c, interzone; b, fixation. Bars = 200 µm. (D) to (F) Closer view in the fixation zone of M. truncatula nodules. DNA was stained using DAPI (blue). (D) MtMOT1.3-HA signal. (E) *S. meliloti* signal. (F) Overlay of MtMOT1.3-HA, *S. meliloti* and DNA signals. Bars = 50 µm. (G) to (I) Transient co-expression of MtMOT1.3-GFP and plasma membrane marker-CFP in *N. benthamiana* leaves. (G) MtMOT1.3-GFP signal. (H) Plasma membrane marker-CFP signal. (I) Overlay of MtMOT1.3-GFP, plasma membrane marker-CFP signals and differential interference contrast. Bars = 25 µm.

Figure 5. *MtMOT1.3* mutation results in a reduced nitrogen fixation rate. (A) Position of the *Tnt1* insertion within the *MtMOT1.3* genomic region. (B) RT-PCR amplification of *MtMOT1.3* transcript in 28 dpi nodules of *M. truncatula* wild type (WT) and mutant (*mot1.3-1*) plants. *Ubiquitin carboxyl-terminal hydrolase1* (*MtUb1*) was used as control for PCR amplifications. (C) Growth of representative plants of wild type, *mot1.3-1* mutant and *mot1.3-1* mutant transformed with the *MtMOT13-HA* construct. Bar = 3 cm. (D) Dry weight of shoots and roots. Data are the mean ± SD of at least 6 independently transformed plants. Asterisk indicates significant differences: **$p < 0.01$, ***$p < 0.005$. (E) Nitrogenase activity in 28-dpi nodules. Acetylene reduction was measured in duplicate from two sets of four pooled plants. Data are the mean ± SD. (F) Number of nodules per plant. Data are the mean ± SD of at least 6 independently transformed plants. (G) Representative nodules of each *M. truncatula* line. Bar = 500 µm. (H) Molybdenum content in shoots, roots, and nodules of wild type, *mot1.3-1* mutant, and *mot1.3-1* mutant transformed with the *MtMOT13-HA* construct. Data are the mean ± SD of 3 sets of 4 pooled plants.

Figure 6. *mot1.3-1* mutant phenotype is not present in non-symbiotic conditions. (A) Growth of representative plants of wild type and *mot1.3-1* mutant. Bar = 3 cm. (B) Dry

bioRxiv preprint doi: https://doi.org/10.1101/102517; this version posted January 24, 2017. The copyright holder for this preprint (which was not certified by peer review) is the author/funder, who has granted bioRxiv a license to display the preprint in perpetuity. It is made available under aCC-BY-NC-ND 4.0 International license.

weight of shoots and roots. Data are the mean ± SD of at least 8 independent plants. (C) Nitrate reductase activity. Nitrate reduction was measured in duplicate. Data are the mean ± SD.

Figure 7. Proposed model for MtMOT1.3 function in molybdenum homeostasis in *M. truncatula*. Molybdenum, in form of molybdate would be released in the infection/differentiation zone, as already described for iron, in a process that could be assisted by a yet-to-be identified transporter that might belong to the MOT1 family (MtMOT1.X). From this point MtMOT1.3 would introduce molybdate into the cytoplasm of infected and non-infected cells within the nodule. The molybdate transport across the symbiosome membrane could be mediated by an orthologue of *L. japonicus* sulfate transporter SST1. Finally, molybdate would entry the bacteroids through the membrane component of the bacterial high affinity molybdate transport system ModB. IM, bacteroid inner membrane; OM, bacteroid outer membrane; SM, symbiosome membrane; PM, nodule cell plasma membrane.

bioRxiv preprint doi: https://doi.org/10.1101/102517; this version posted January 24, 2017. The copyright holder for this preprint (which was not certified by peer review) is the author/funder, who has granted bioRxiv a license to display the preprint in perpetuity. It is made available under aCC-BY-NC-ND 4.0 International license.

Figure 1

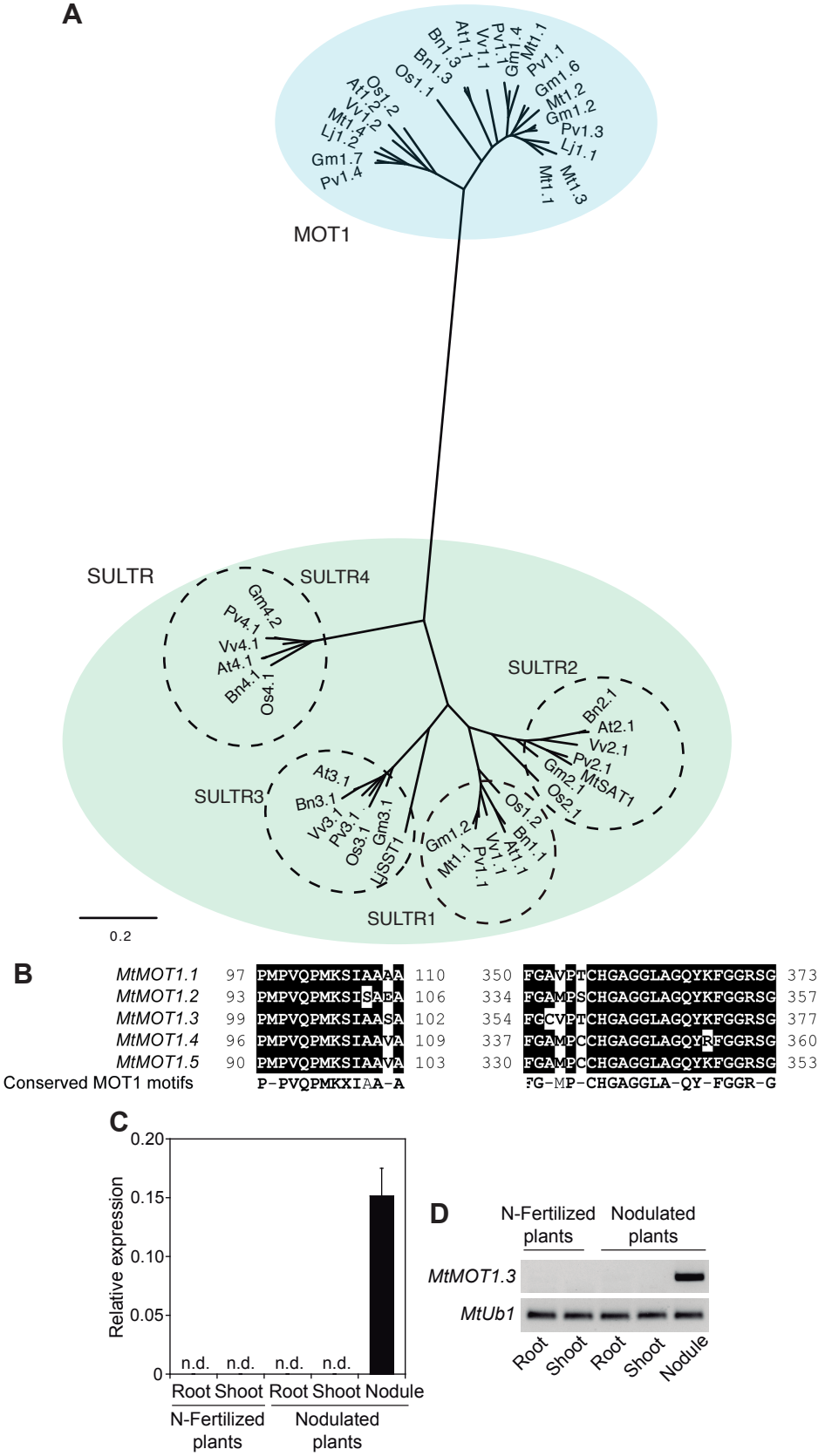

Figure 1. MtMOT1.3 is a member of the MOT1 protein and is expressed in the nodule.
(A) Unrooted tree of the plant SULTR and MOT1 families. (B) Alignment of the conserved motifs of the MOT1 proteins present in all *M. truncatula* MOT1 members. Sequence were aligned using ClustalW method and it is extracted from a larger alignment including the full protein sequence of the M. truncatula MOT1 members. (C) and (D) Determination of *MtMOT1.3* expression in nodulated and nitrogen-fertilized M. truncatula plants relative to the internal standard gene *Ubiquitin carboxyl-terminal hydrolase*. Data are the mean ± SD of two independent experiments with 4 pooled plants. n.d., non-detected. (D) *MtMOT1.3* expression in nodulated and nitrogen-fertilized *M. truncatula* plants. *Ubiquitin carboxyl-terminal hydrolase1* (*MtUb1*) was used as control for PCR amplifications.

bioRxiv preprint doi: https://doi.org/10.1101/102517; this version posted January 24, 2017. The copyright holder for this preprint (which was not certified by peer review) is the author/funder, who has granted bioRxiv a license to display the preprint in perpetuity. It is made available under aCC-BY-NC-ND 4.0 International license.

Figure 2

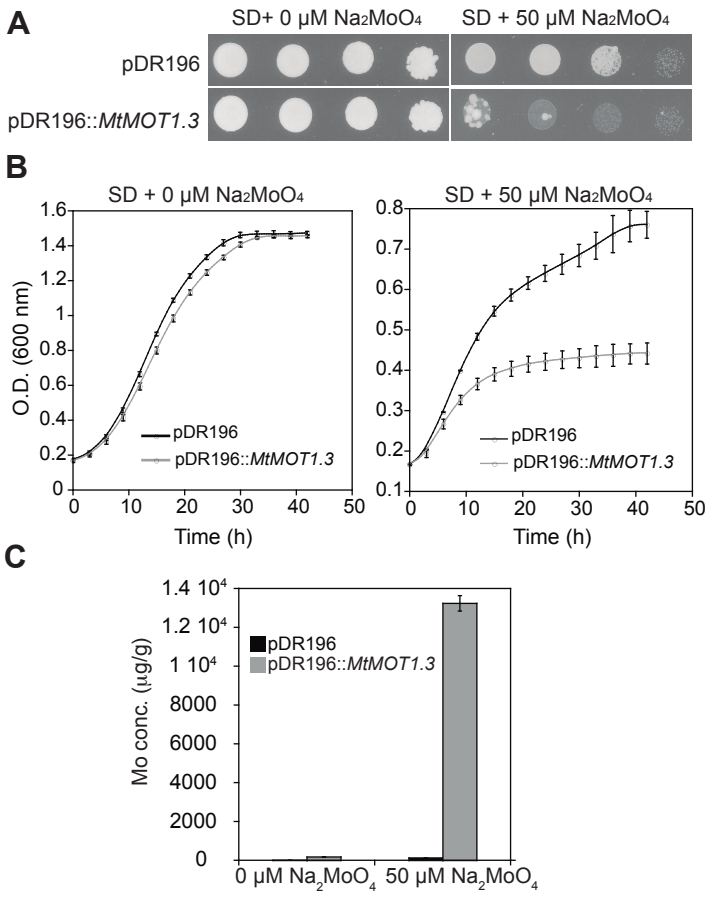

Figure 2. MtMOT1.3 transports molybdate towards the cytosol. (A) *S. cerevisiae* strain 31019b was transformed with PDR196 empty vector or PDR196 containing *MtMOT1.3* coding sequence, and grown at 28 ºC for 3d in serial dilution (10X) on SD solid medium medium without an added molybdenum source or containing 50 µM sodium molybdate. (B) *S. cerevisiae* strains used in (A) were grown in SD liquid medium, with and without 50 µM sodium molybdate, at 28 ºC for 42 h. Yeast growth was monitored by measuring optical density at 600 nm every 3h. (C) Molybdenum content in the yeast grown in (B) after 42 h. Data are the mean ± SD of two independent experiments.

bioRxiv preprint doi: https://doi.org/10.1101/102517; this version posted January 24, 2017. The copyright holder for this preprint (which was not certified by peer review) is the author/funder, who has granted bioRxiv a license to display the preprint in perpetuity. It is made available under aCC-BY-NC-ND 4.0 International license.

Figure 3

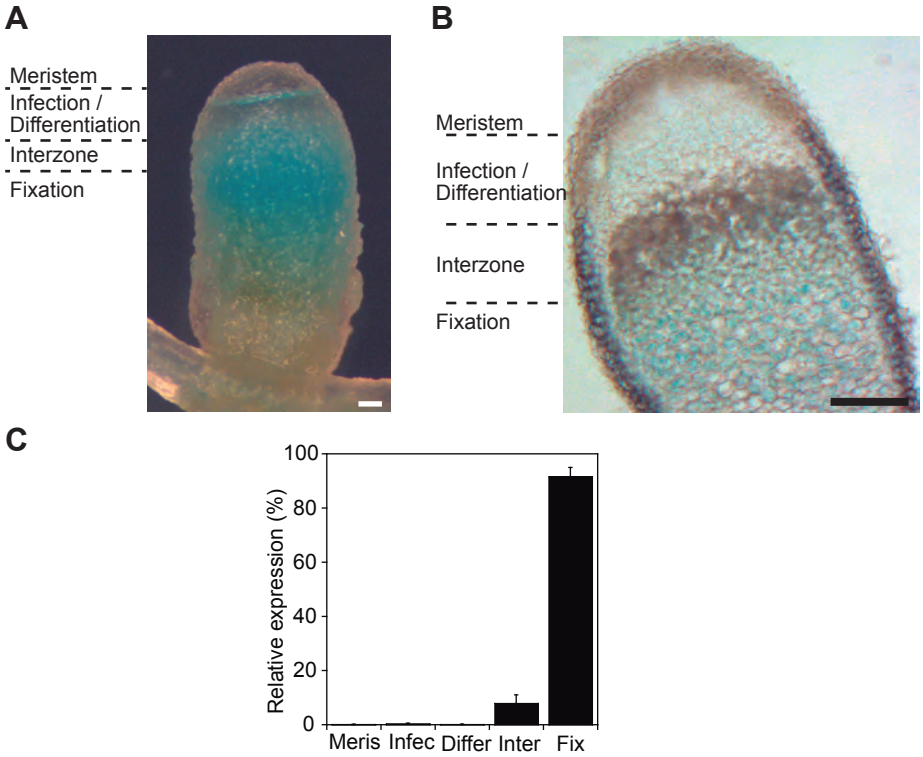

Figure 3. *MtMOT1.3* gene is expressed in the interzone and fixation zone of *M. truncatula* nodules. (A) and (B) GUS staining of *M. truncatula* 28-dpi nodules transiently expressing gus gene under the control of *MtMOT1.3* promoter. (A) Intact nodule. (B) Longitudinal nodule section. Bars = 200 µm. (C) Expression of *MtMOT1.3* in *M. truncatula* nodules by laser-capture microdissection coupled to RNA sequencing. Data were obtained from the Symbimics database (https://iant.toulouse.inra.fr/symbimics/). Meris, meristem; Infec, infection zone; Differ, differentiation zone; Inter, interzone; Fix, fixation zone.

bioRxiv preprint doi: https://doi.org/10.1101/102517; this version posted January 24, 2017. The copyright holder for this preprint (which was not certified by peer review) is the author/funder, who has granted bioRxiv a license to display the preprint in perpetuity. It is made available under aCC-BY-NC-ND 4.0 International license.

Figure 4

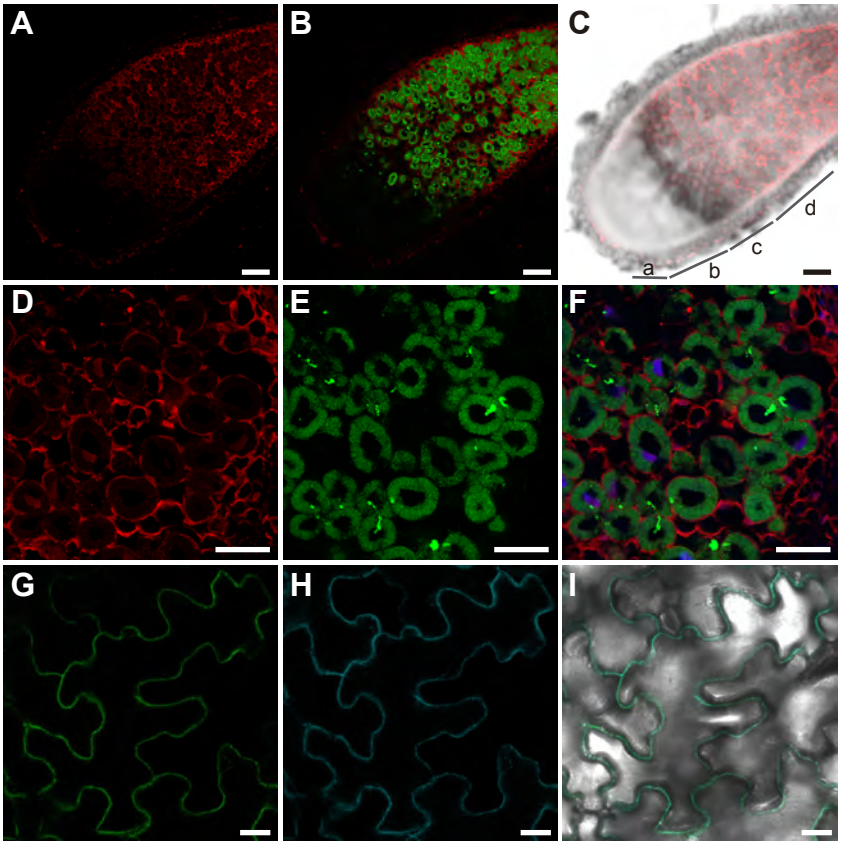

Figure 4. MtMOT1.3 is localized in the plasma membrane. (A) to (C) Cross section of a 28-dpi *M. truncatula* nodule transiently expressing MtMOT1.3-HA construct and infected with a *S. meliloti* strain constitutively expressing GFP (green). MtMOT1.3-HA was detected using an Alexa-594-conjugated antibody (red). (A) MtMOT1.3-HA signal. (B) Overlay of MtMOT1.3-HA and *S. meliloti* signals. (C) Overlay of MtMOT1.3-HA signal and differential interference contrast. a, meristem; b, infection/differentiation; c, interzone; d, fixation. Bars = 200 µm. (D) to (F) Closer view in the fixation zone of *M. truncatula* nodules. DNA was stained using DAPI (blue). (D) MtMOT1.3-HA signal. (E) *S. meliloti* signal. (F) Overlay of MtMOT1.3-HA, *S. meliloti* and DNA signals. Bars = 50 µm. (G) to (I) Transient co-expression of MtMOT1.3-GFP and plasma membrane marker-CFP in *N. benthamiana* leaves. (G) MtMOT1.3-GFP signal. (H) Plasma membrane marker-CFP signal. (I) Overlay of MtMOT1.3-GFP, plasma membrane marker-CFP signals and differential interference contrast. Bars = 25 µm.

bioRxiv preprint doi: https://doi.org/10.1101/102517; this version posted January 24, 2017. The copyright holder for this preprint (which was not certified by peer review) is the author/funder, who has granted bioRxiv a license to display the preprint in perpetuity. It is made available under aCC-BY-NC-ND 4.0 International license.

Figure 5

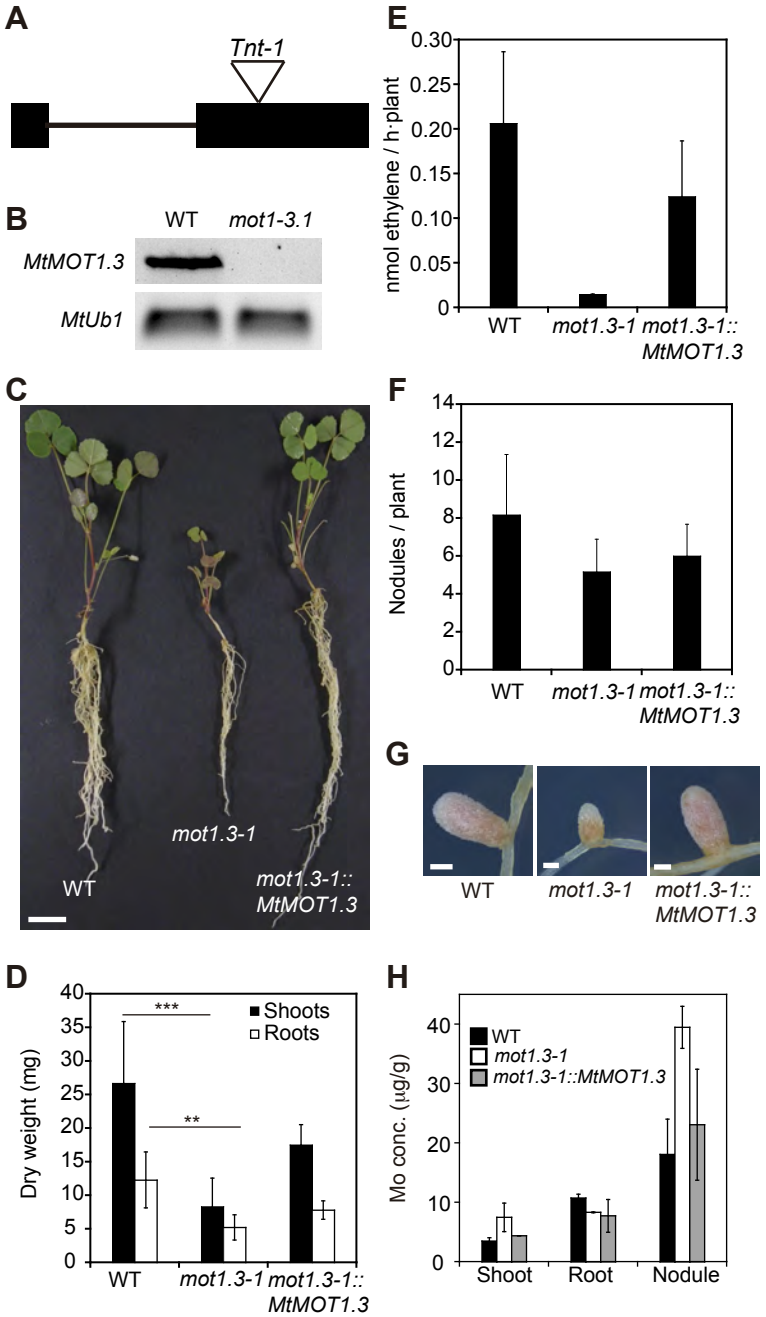

Figure 5. *MtMOT1.3* mutation results in a reduced nitrogen fixation rate. (A) Position of the *Tnt1* insertion within the *MtMOT1.3* genomic region. (B) RT-PCR amplification of *MtMOT1.3* transcript in 28 dpi nodules of *M. truncatula* wild type (WT) and mutant (*mot1.3-1*) plants. *Ubiquitin carboxyl-terminal hydrolase1* (*MtUb1*) was used as control for PCR amplifications. (C) Growth of representative plants of wild type, *mot1.3-1* mutant, and *mot1.3-1* mutant transformed with the *MtMOT13-HA* construct. Bar = 3 cm. (D) Dry weight of shoots and roots. Data are the mean ± SD of at least 6 independently transformed plants. Asterisk indicates significant differences: **$p < 0.01$, ***$p < 0.005$. (E) Nitrogenase activity in 28-dpi nodules. Acetylene reduction was measured in duplicate from two sets of four pooled plants. Data are the mean ± SD. (F) Number of nodules per plant. Data are the mean ± SD of at least 6 independently transformed plants. (G) Representative nodules of each *M. truncatula* line. Bar = 500 µm. (H) Molybdenum content in shoots, roots, and nodules of wild type, *mot1.3-1* mutant, and *mot1.3-1* mutant transformed with the *MtMOT13-HA* construct. Data are the mean ± SD of 3 sets of 4 pooled plants.

bioRxiv preprint doi: https://doi.org/10.1101/102517; this version posted January 24, 2017. The copyright holder for this preprint (which was not certified by peer review) is the author/funder, who has granted bioRxiv a license to display the preprint in perpetuity. It is made available under aCC-BY-NC-ND 4.0 International license.

Figure 6

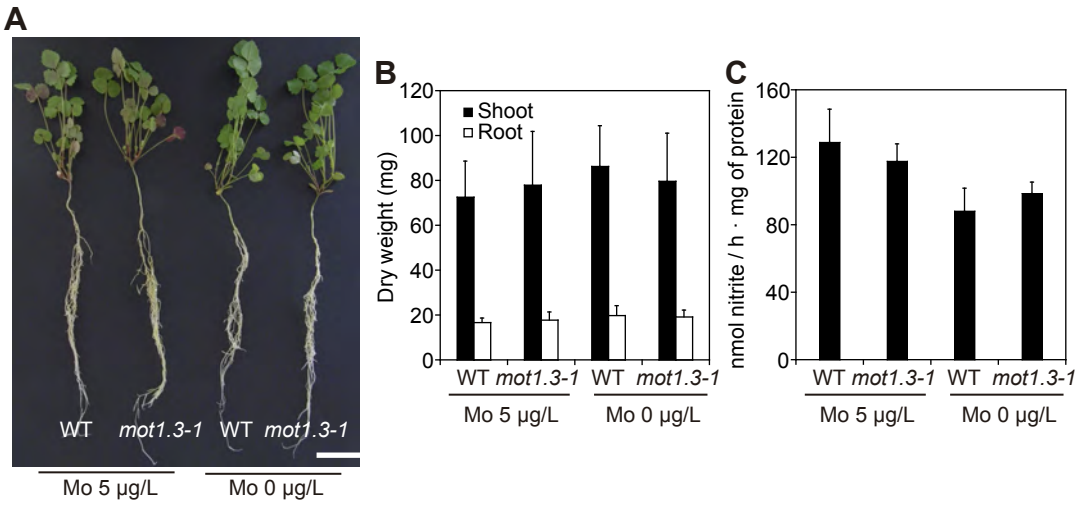

Figure 6. *mot1.3-1* mutant phenotype is not present in non-symbiotic conditions. (A) Growth of representative plants of wild type and *mot1.3-1* mutant. Bar = 3 cm. (B) Dry weight of shoots and roots. Data are the mean ± SD of at least 8 independent plants. (C) Nitrate reductase activity. Nitrate reduction was measured in duplicate. Data are the mean ± SD.

bioRxiv preprint doi: https://doi.org/10.1101/102517; this version posted January 24, 2017. The copyright holder for this preprint (which was not certified by peer review) is the author/funder, who has granted bioRxiv a license to display the preprint in perpetuity. It is made available under aCC-BY-NC-ND 4.0 International license.

Figure 7

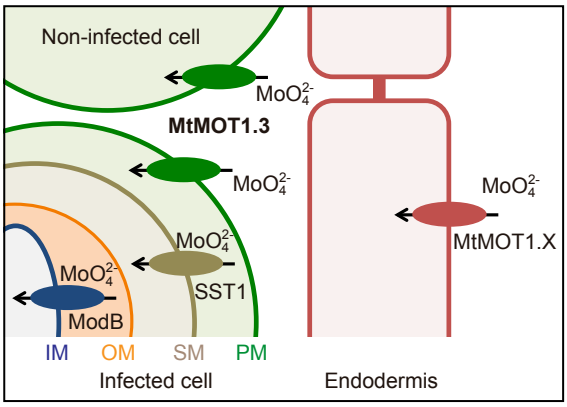

Figure 7. Proposed model for MtMOT1.3 function in molybdenum homeostasis in *M. truncatula*. Molybdenum, in form of molybdate would be released in the infection/differentiation zone, as already described for iron, in a process that could be assisted by a yet-to-be identified transporter that might belong to the MOT1 family (MtMOT1.X). From this point MtMOT1.3 would introduce molybdate into the cytoplasm of infected and non-infected cells within the nodule. The molybdate transport across the symbiosome membrane could be mediated by an orthologue of *L. japonicus* sulfate transporter SST1. Finally, molybdate would entry the bacteroids through the membrane component of the bacterial high affinity molybdate transport system ModB. IM, bacteroid inner membrane; OM, bacteroid outer membrane; SM, symbiosome membrane; PM, nodule cell plasma membrane.